Bulletin of Mathematical Biology (2004)
doi:10.1016/j.bulm.2003.11.008

Effect of Heterogeneous Structure in Mechanically Unstressed Biofilms on Overall Growth

I. KLAPPER
Department of Mathematical Sciences and Center for Biofilm Engineering,
Montana State University,
Bozeman, MT 59717,
USA
E-mail: klapper@math.montana.edu

In contrast to their name, biofilms are not always flat and homogeneous but instead often exhibit complex structural heterogeneity. It has been suggested that nonhomogeneous geometry is selected in order to increase biofilm growth rate. A previous study (Dockery and Klapper (2002) *SIAM J. Appl. Math.*, **62**, 853–869) of a model biofilm system in a static bulk fluid demonstrated that under some circumstances a flat biofilm–bulk fluid interface is linearly unstable to perturbation due to growth induced forces. Computations indicated that subsequent nonlinear evolution results in fingers and mushrooms of biofilm similar to structures observed in actual biofilms. However, the important complementary issue of biological functionality was not considered. Here a weakly nonlinear analysis of the simple growing biofilm layer model in Dockery and Klapper (2002, *SIAM J. Appl. Math.*, **62**, 853–869) is presented. It is argued that, at least in the case of biofilms free of external mechanical stress, overall growth is in fact generally inhibited by the presence of growing perturbations in the linear stage. Hence a more complex explanation of function is necessary.

1. INTRODUCTION

A biofilm is a hydrated collection of microorganisms concentrated together in a self-secreted matrix of extracellular polymeric substances (EPS). Biofilms are nearly ubiquitous in damp and wet environments, and, in fact, the majority of bacteria in natural and pathogenic systems are located within biofilm systems (Costerton *et al.*, 1987, 1999). Examples include, among many others, pipe scum in water and industrial systems, dental plaque, algal mats, and waste-water treatment systems. Biofilm presence has important medical consequences; they are responsible for chronic infections such as gum disease, recurring ear infections, lung infections in sufferers of cystic fibrosis, and skin infections in severe burn victims, again among many other examples. See Costerton (1995), Breyers (2000) and Stoodley *et al.* (2002) for an overview. Biofilms demonstrate a variety of remarkable behaviors including complex responses to environmental conditions though little is known

0092-8240/04/000001 + 16 $30.00/0

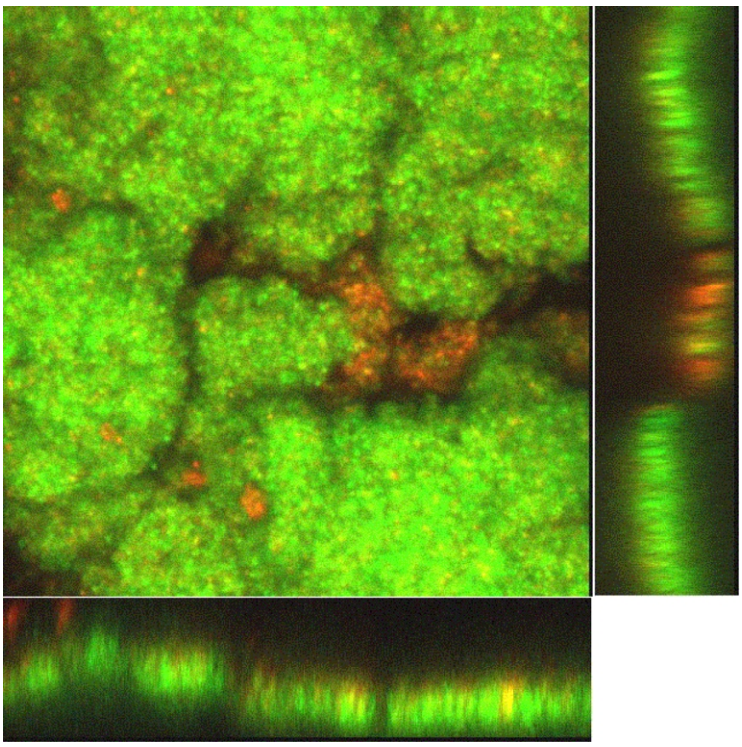

Figure 1. Confocal image of *Streptococcus mutans* biofilm grown in a drip flow reactor as in Heersink *et al*. (2003). The main panel is a plan view (350 μm^2); the side and bottom panels are vertical cross-sections through the biofilm of the plan view cut in, respectively, the top–bottom and left–right directions. *S. mutans* is an early colonizer of teeth and is one of the causative agents of caries through acid production. Image supplied courtesy of Joanna Heersink and Paul Stoodley, Center for Biofilm Engineering, Montana State University.

about their mechanical and chemical properties. Yet an understanding of form and function of biofilm structure is essential for progress in important problems like biofilm control.

Biofilms are observed to exhibit heterogeneous morphologies in general (Fig. 1). How and why spatial nonuniformities develop is not understood. Varied explanations have been proposed for formation of structures such as mushrooms and channels including chemical, hydrodynamical, and mechanical mechanisms. As mechanical forces will always be present regardless, it seems a useful exercise to study consequences of mechanics in the absence of other influences. A number of modeling attempts have essentially taken this point of view (Wanner and Riechert, 1996; Wimpenny and Colasanti, 1997; Heijnen *et al*., 1998; Wood and Whitaker, 1999; Picioreanu, 2000; Eberle *et al*., 2001; Hermanowicz, 2001; Kreft and Wimpenny, 2001; Dockery and Klapper, 2002; Cogan, 2003). In an earlier paper (Dockery and Klapper, 2002) (hereafter referred to as DK02), it was argued using a rather general continuum mechanics model that internally generated

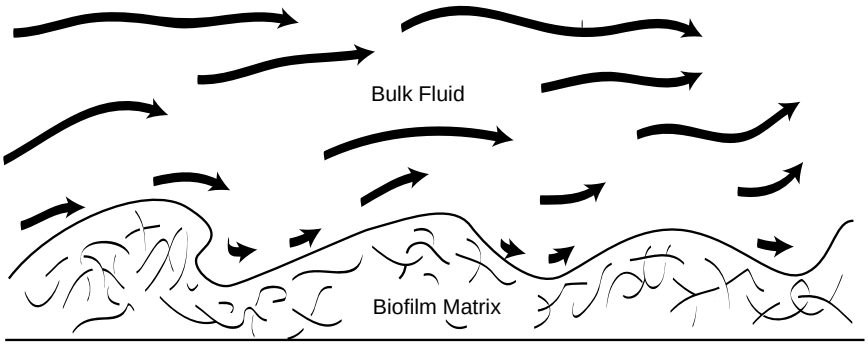

Figure 2. Cartoon of a biofilm–bulk fluid system. Bulk fluid flow above the biofilm–bulk fluid interface provides a source of substrates for the biofilm as well as imparting mechanical stress. Individual entangled EPS polymer chains are depicted within the biofilm matrix [after Koerstgens *et al*. (2001)].

mechanical stress from growth alone can explain at least some aspects of biofilm structure formation. Other investigators have reached the same conclusion using cellular automata based methods. This paper, a sequel to DK02, focuses on one key consequence of biofilm structure in the same simplified setting of absence of externally imposed mechanical stress—are biofilm fingers and mushrooms favorable for biofilm growth?

Biofilms are often found as a thin layer attached to a solid substratum within a dynamic aqueous environment, the bulk fluid (Fig. 2). Nutrients (substrates) are delivered to the biofilm from the bulk fluid, typically through a combination of advection and diffusion. The bulk fluid also interacts mechanically with the biofilm through transmitted shear stress. This influence is complex; biofilms appear to behave as viscoelastic fluids (Klapper *et al*., 2002; Towler *et al*., in press). Conversely, despite the extreme thinness of biofilms, their viscoelastic response can have dramatic effects on the bulk fluid flow (Schultz and Swain, 1999). Detailed understanding of biofilm material properties and their consequences are lacking at the current time. However, the analysis presented here restricts to the case of static or nearly static bulk fluid and thus direct consequences of shear stress conveyance and associated viscoelastic response are avoided. A second consequence of this simplification is that substrates are delivered through the bulk fluid diffusively only. Layer thicknesses are generally $O(10^2\ \mu\mathrm{m})$ or less. Within the biofilm, microorganisms gain access to substrates through diffusion, usually from the bulk fluid. On the laboratory timescale, diffusion over $O(10^2\ \mu\mathrm{m})$ lengths is fast. Nevertheless, despite the layer thinness, certain substrates may be consumed before penetration through the entire biofilm can occur (Wentland *et al*., 1996; Xu *et al*., 1998). In this case an active layer is formed adjacent to the biofilm–bulk fluid interface in the region where a limiting substrate is still available before being largely depleted further into the biofilm. Below this layer, little activity occurs. In DK02, a linear analysis of a continuum biofilm model indicated that a flat biofilm

interface could be subject to growth induced instabilities on wavelengths of the lengthscale of the active layer depth. Computational investigation of the nonlinear evolution of these instabilities showed formation of finger and mushroom-like structures extending into the bulk fluid. Similar structures are often observed in actual biofilms, provoking obvious questions of biological function. For example, does the increased surface area of a fingered biofilm–bulk fluid interface promote overall growth rate? Numerical studies of several models seem to indicate not. It is argued here that, within the linear regime and in the absence of significant advective flow in the bulk fluid, interface structure generally does not enhance overall biofilm growth but on the contrary would seem to suppress it somewhat. As mentioned, numerics of various models have already supported that conclusion in the nonlinear regime. The analysis presented in DK02 fails to address this question because in the linear theory, mean growth is unchanged to first order by an interface perturbation. Hence a second order analysis becomes necessary. In passing it is noted that a weakly nonlinear analysis of a related tumor growth model was performed in Byrne (1999) with the purpose of identifying nontrivial steady solutions. In fact, the biofilm model presented in DK02 bears similarities to a number of tumor growth models (Greenspan, 1974, 1975; Chaplain *et al*., 1995; Byrne, 1999).

It should be stated that the presence of nonnegligible advective transport may effect the conclusions presented here. Delivery of substrate deep into the biofilm through advection may very well be an important factor in biofilm growth in those biofilms exposed to such flows, possibly sufficiently important so as to change some of the conclusions of this paper in such cases. However, such flow can also be expected to exert significant mechanical stress on the biofilm, stress that might exert as important or more important an influence on biofilms as advective delivery of substrates. Biofilm mechanics are not sufficiently understood at this moment to be included in the present model and hence this regime is beyond consideration here.

2. THE MODEL

2.1. ***The model equations.*** We rely on a continuum model [dating at least to Greenspan's tumor growth models (Greenspan, 1974, 1975)] consisting of a biofilm matrix of EPS plus microorganisms of density $\rho(\mathbf{x}, t)$ and velocity $\mathbf{v}(\mathbf{x}, t)$ together with a growth source depending on a single limiting substrate concentration $S(\mathbf{x}, t)$. Space is divided into 2 regions: a biofilm region W_B and a bulk fluid region W_F (Fig. 3). For the purposes of the small perturbations considered in this paper it is allowable to assume that the biofilm–bulk fluid interface can be represented in the form $z = h(x, y, t)$. Within the bulk fluid, S diffuses and (in general) advects; within the biofilm S diffuses, (in general) advects, and is consumed according to a usage function $u(S)$. Due to the fact that the evolution timescale of

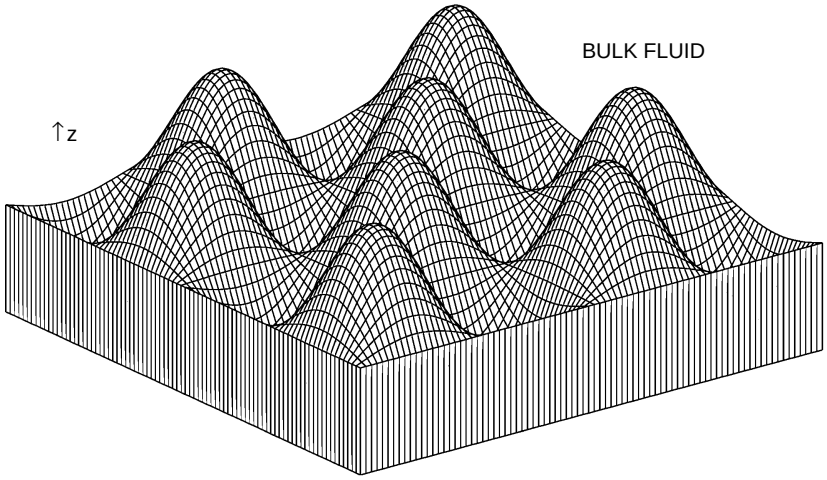

Figure 3. Slab of biofilm (region W_B) below the bulk fluid (region W_F). The biofilm extends to $z = -\infty$. The extent of the bulk fluid region W_F in z is finite.

the biofilm (hours) is extremely long compared to the diffusive timescale (seconds), at any given instant one can assume that the substrate concentration is at equilibrium. Also, for the very small velocities to be considered here, advective effects can be disregarded. Under these approximations, in nondimensional form the substrate concentration diffusion equation takes the form (DK02):

$$\nabla^2 S = \begin{cases} 0 & \text{bulk flow region} \\ Gu(S) & \text{biofilm region.} \end{cases} \tag{1}$$

$G = \mathcal{L}^2 u(S_\infty)/\kappa S_\infty$ is a nondimensional parameter measuring, roughly, the square of the ratio of the system lengthscale $\mathcal{L}$ to the biofilm active layer depth $\kappa S_\infty/u(S_\infty)$, the depth to which substrate can penetrate before being appreciably consumed. S_∞ is a representative value of S, say the boundary condition on S at the top of the bulk fluid region, and κ is the substrate diffusivity within the biofilm. Large G corresponds to, for example, low substrate level. Note that substrate diffusivity generally differs between bulk fluid and biofilm; however the difference is not large [typically $1 < \kappa_{\text{bulk}}\kappa_{\text{biofilm}}^{-1} < 5$ depending on the physical properties of the substrate and also on details of the biofilm geometry and structure (Stewart, 2003)] and only a more substantial variation in κ would have a qualitative effect on the results reported here. Hence for simplicity it will be assumed that diffusivity is constant throughout the entire domain. Completing the boundary and interface conditions, note that substrate concentration S satisfies no flux conditions at the bottom of the biofilm region and continuity conditions at the interface between biofilm and bulk fluid, i.e., $[S] = [\nabla S \cdot \mathbf{n}] = 0$. Also, for later use, define a second nondimensional parameter $F = \ell(u(S_\infty)/\kappa S_\infty)^{1/2}$, where ℓ is a characteristic depth of the substrate boundary layer in W_F adjacent to the biofilm interface.

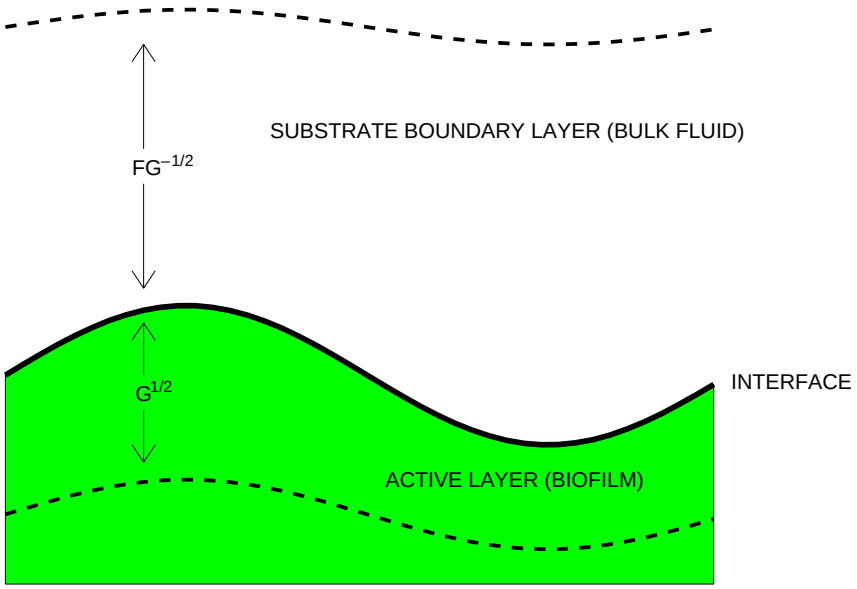

Figure 4. Shaded region is biofilm and unshaded region is bulk fluid. If distances are scaled by the system size $\mathcal{L}$ then the active biofilm layer is approximately of depth $G^{-1/2}$. Across the interface from the biofilm is a bulk fluid boundary layer through which substrate diffuses; this layer has depth $\ell/\mathcal{L} = FG^{-1/2}$, i.e., F is the ratio of the substrate boundary layer depth to the biofilm active layer depth. Above the substrate boundary layer resides bulk fluid with full value of substrate concentration.

F measures the ratio of the bulk fluid region boundary layer depth to the active region depth and is related to G by $F = (\ell/\mathcal{L})\sqrt{G}$ (Fig. 4). In the case of an unstable perturbation to the biofilm–bulk fluid interface, as will be discussed later, the most unstable wavelength k^{-1} is proportional to the active layer depth. Hence in the unstable regime, F also measures the ratio of the bulk fluid boundary layer depth to the instability lengthscale.

We regard biofilm as a matrix of density ρ contained in a bath of mostly water (biofilms are generally 90% or more water by mass or volume). Consumption of substrate results in growth of new biofilm matrix at a source rate given by a function $g(u(S))$. Thus within W_B

$$\rho_t + \nabla \cdot (\rho \mathbf{v}) = \rho g. \tag{2}$$

Though there is evidence that matrix density ρ varies in response to environment, in the present context of slow growth and steady environmental conditions we assume that ρ is constant, i.e., the biofilm matrix is incompressible, so that $\nabla \cdot \mathbf{v} = g$.

Typical choices for u and g are $g(u) = \beta u$ and $u(S) = \alpha S$ (linear kinetics) or $u(S) = \alpha S(\beta + S)^{-1}$ (Monod kinetics) but in fact u and g are unknown and may be expected to vary from one biofilm system to another. As substrate-limiting environments are most relevant to interface fingering instabilities of the form considered here (see DK02), we will later simplify by taking the linear approximations

to u and g around $S = 0$, i.e., $u(S) = S$, $g(u) = u = S$ (noting that the coefficients α and β can be scaled to 1 without loss of generality). More generally g might take the form $g(u(S)) = S - \gamma$ where γ is a death rate parameter, but the presence or absence of this extra term does not affect the results reported here.

The momentum equation in W_B takes the usual form

$$(\rho \mathbf{v})_t + \nabla \cdot (\rho \mathbf{v} \otimes \mathbf{v}) = \nabla \cdot \boldsymbol{\sigma} \tag{3}$$

where $\boldsymbol{\sigma}$ is the stress tensor for the biofilm matrix. The inertial term $\nabla \cdot (\rho \mathbf{v} \otimes \mathbf{v})$ can be neglected here, while the noninertial stress $\boldsymbol{\sigma}$ can be broken into 4 pieces

$$\boldsymbol{\sigma} = \boldsymbol{\sigma}_h + \boldsymbol{\sigma}_d + \boldsymbol{\sigma}_p + \boldsymbol{\sigma}_b$$

where $\boldsymbol{\sigma}_h$ is the hydrostatic pressure stress, $\boldsymbol{\sigma}_d$ is the deviatoric viscoelastic stress [see Klapper *et al.* (2002)], $\boldsymbol{\sigma}_p$ is the osmotic matrix pressure, and $\boldsymbol{\sigma}_b$ is Brownian friction stress. We assume due to the thinness of the biofilm layer [$O(10^2\ \mu\text{m})$] and slow growth time [$O(10^4\ \text{s})$] that hydrostatic pressure disturbances equilibrate on timescales much shorter than those of interest and hence $\boldsymbol{\sigma}_h$ can be neglected. Similarly, $\boldsymbol{\sigma}_d$ can be argued to be negligible relative to $\boldsymbol{\sigma}_b$ as follows: first, since the biofilm growth time [$O(10^4\ \text{s})$] is large compared to the elastic relaxation time [$O(10^2\ \text{s})$, see Klapper *et al.* (2002)] then the elastic component of $\boldsymbol{\sigma}_d$ is unimportant. Second, to compare the frictional stresses contributed by $\boldsymbol{\sigma}_d$ and $\boldsymbol{\sigma}_b$, note that the systematic growth induced biofilm velocities are of order (biofilm height/growth time) $\sim 10^{-4}\ \text{cm}/10^4\ \text{s} = 10^{-8}\ \text{cm s}^{-1}$ whereas the fluctuating Brownian velocities are of order $\sqrt{kT} \sim 10^{-6}\ \text{cm s}^{-1}$ with shorter spatial scales. Thus $\boldsymbol{\sigma}_d$ can be neglected in favor of $\boldsymbol{\sigma}_b$. However, over time, stress from $\boldsymbol{\sigma}_b$ averages to 0 whereas osmotic pressure will increase as biofilm matrix is produced by new growth until $\boldsymbol{\sigma}_p$ is significant relative to $\boldsymbol{\sigma}_b$ and so $\boldsymbol{\sigma}_p$ should not be disregarded. If then we integrate over a time long compared to Brownian motion time correlations but short compared to growth time, without trying to rigorously justify, we assume that we obtain a Darcy's law

$$\mathbf{v} = \alpha \nabla \cdot \boldsymbol{\sigma}_p = -\alpha \nabla_p \tag{4}$$

for some proportionality constant α, where p is the osmotic pressure. Combined with incompressibility this implies

$$\alpha \nabla^2 p = -g. \tag{5}$$

In the absence of flow in W_F we can set $p = 0$ at the interface. Also (4) requires $dp/dn = 0$ at the bottom of the biofilm region.

Cogan (2003) used a similar model except with a Navier–Stokes stress balance $\mu \nabla^2 \mathbf{v} = \alpha \nabla p$ instead of the Darcy's law (4). Results of the linear analysis for that

model are qualitatively similar to those in DK02. Use of the Navier–Stokes balance would also not qualitatively affect the weakly nonlinear analysis presented here. The reason for this is that biofilm evolution in this model is mainly determined by the substrate profile $S(\mathbf{x}, t)$ [which in turn determines the growth profile $g(S)$] together with incompressibility $\nabla \cdot \mathbf{v} = g$. Both are independent of the stress balance equation.

To complete the model system, given the pressure profile p the biofilm interface moves at velocity $-\alpha \nabla p \cdot \mathbf{n}$ where $\mathbf{n}$ is the unit normal out of W_B. Note that (5) implies that p is proportional to α^{-1} and thus that $\mathbf{v}$ (and the interface velocity) is independent of α. Hence α can be removed from the problem. Having done so, the interface $z = h$ moves according to

$$\nabla^2 p = -g \tag{6}$$

$$\frac{dh}{dt} = -(\nabla p \cdot \mathbf{n})(\hat{\mathbf{z}} \cdot \mathbf{n}) \tag{7}$$

where $\hat{\mathbf{z}}$ is a unit vector in the z-direction.

For simplicity the depth of the biofilm region W_B is allowed to be infinite. Results for the infinite depth biofilm are close to those for a finite depth biofilm as long as the depth of the finite biofilm is sufficiently large compared to the depth $(u(S_\infty)/\kappa S_\infty)^{-1/2}$ of the active region (see DK02), a reasonable assumption for a typical 100 μm deep biofilm in substrate limited conditions.

2.2. ***Zeroth and first order results.*** One dimensional (1D) solutions and their linear stability analysis for the system (1), (6) and (7) were presented in DK02. Those results are briefly summarized here. First, if initial conditions depend only on z then the solution of the biofilm equations remains one dimensional for all later times. If it is assumed that a renewable substrate source lies above the top of a bulk fluid region W_F and thus that W_F as a whole comprises a substrate boundary layer with a constant in time thickness L (in nondimensional units, i.e., scaled by a system lengthscale $\mathcal{L}$) then 1D solutions take the form $h = h^{(0)}(t) = h^{(0)}(0) + ct$ for a particular c, $S = S^{(0)}(z, t) = S^{(0)}(z - h^{(0)}(t))$, and $p = p^{(0)}(z, t) = p^{(0)}(z - h^{(0)}(t))$, i.e., the interface velocity is constant and the substrate and pressure profiles are steady in the frame moving with the interface. Also, it was shown that this zeroth order solution is linearly unstable to small initial perturbations $h(x, y, 0) = h^{(0)}(0) + (H_1 e^{i\mathbf{k}\cdot\mathbf{x}} + c.c.)$, $\mathbf{k} = (k_1, k_2)$, $\mathbf{x} = (x, y)$, of the interface for sufficiently large values of the dimensionless number G.

However, the linear analysis presented in DK02 was unable to address at least one important issue, namely the question of how nonuniform structure affects mean biofilm growth. Does an interface help or hinder uptake and usage of substrate? In order to preserve biomass, the initial perturbation to h necessarily must have zero mean displacement. To first order, this initial condition is preserved for all

later times in all quantities including, notably, total growth of new biofilm matrix. In particular, to first order

$$\int_{W_B} g\, d\mathbf{x} = \int_{W_B} (g^{(0)} + g^{(1)}) d\mathbf{x} = \int_{W_B} g^{(0)} d\mathbf{x}$$

where $g^{(0)}$, $g^{(1)}$ are defined by $g(u(S^{(0)} + S^{(1)})) \cong g(u(S^{(0)})) + g'(u(S^{(0)}))S^{(1)} \equiv g^{(0)} + g^{(1)}$, and $S^{(1)}$ is the first order correction to substrate density. Thus from the point of view of total biofilm growth, linear analysis is neutrally stable and therefore it becomes necessary to extend to second order to address the question of effect of fingering structure on biofilm growth.

Hence we consider a second order analysis in the following section in order to address this question. The nature of the analysis differs from many weakly nonlinear studies, e.g., Ermentrout (1991), in that the important nonlinearity in the system is due to the moving interface and not due to nonlinear terms in the actual equations (or boundary conditions). In fact the most relevant regime is that of low substrate concentration for which one can safely replace the usage and growth functions u, g, by linear approximations. In this case the model equations themselves are in fact linear and the only nonlinearity occurs due to the interface. As mentioned previously, for simplicity and clarity this assumption will be made throughout the remainder of the paper, in particular we set $u(S) = S$, $g(u) = u$. Having done so it is then possible, see DK02, to explicitly calculate the solutions to (1), (6) and (7).

In particular, at zeroth order

$$S^{(0)}(z,t) = \begin{cases} 1 - \dfrac{F}{1+F}(1 - L^{-1}(z - h^{(0)})) & h^{(0)} < z < h^{(0)} + L \\ \dfrac{1}{1+F}\exp[-\sqrt{G}(h^{(0)} - z)] & z < h^{(0)} \end{cases} \tag{8}$$

$$p^{(0)}(z,t) = G^{-1}\frac{1}{1+F}(1 - \exp[-\sqrt{G}(h^{(0)} - z)]) \qquad z < h^{(0)} \tag{9}$$

$$\frac{dh^{(0)}}{dt} = G^{-1/2}\frac{1}{1+F} \tag{10}$$

and first order,

$$S^{(1)}(z,t) = \begin{cases} -\dfrac{1}{1+F}\dfrac{G}{k + \kappa\tanh(kL)}\dfrac{\sinh[kL(1 - L^{-1}(z - h^{(0)}))]}{\cosh[kL]}h^{(1)}(t) & h^{(0)} < z < h^{(0)} + L \\ -\dfrac{1}{1+F}\dfrac{G\tanh(kL)}{k + \kappa\tanh(kL)}\exp[-\kappa(h^{(0)} - z)]h^{(1)}(t) & -\infty < z < h^{(0)} \end{cases}$$

$$p^{(1)}(z,t) = \frac{1}{1+F}\left(1 + \frac{\sqrt{G}\tanh(kL)}{k + \kappa\tanh(kL)}(e^{-(\kappa - k)(h^{(0)} - z)} - 1)\right)\frac{e^{-k(h^{(0)} - z)}}{\sqrt{G}}h^{(1)}(t) \qquad z < h^{(0)}$$

$$\frac{dh^{(1)}}{dt} = \frac{1}{1+F}\left(1 - \frac{k}{\sqrt{G}} - \frac{G\tanh(kL)}{(k+\kappa)(k + \kappa\tanh(kL))}\right)h^{(1)} \equiv \lambda(k)h^{(1)}$$

where $\kappa^2 = k^2 + G$. For sufficiently large G the perturbation $h^{(1)}$ grows exponentially for some values of k. It is easily checked that the maximum growth rate occurs at $k = O(\sqrt{G})$. In fact, setting $\lambda'(k) = 0$ results in

$$0 = -\frac{1}{\sqrt{G}} + \frac{G\tanh(kL)(1+\tanh(kL))}{\kappa(k+\kappa\tanh(kL))^2} + \frac{GL}{\cosh^2(kL)} \times \frac{\kappa\tanh(kL)(k+\kappa\tanh(kL)) - 1}{k+\kappa\tanh(kL)}. \tag{11}$$

Now, writing $kL = (k/\sqrt{G})(\sqrt{G}L)$ and setting $k_{\max} = C_{\max}\sqrt{G}$, then as G increases we find after some algebra that $k_{\max}$ solves (11) up to an exponentially small correction in $F = \sqrt{G}L$ where $C_{\max} \cong 0.3268$ is the solution of the equation $\sqrt{1+C_{\max}^2}(C_{\max} + \sqrt{1+C_{\max}^2})^2 = 2$. For this value of $k_{\max}$, we obtain $\lambda_{\max} \cong 0.1472$, nearly independent of G for G sufficiently large that F is larger than $O(1)$ for fixed L.

3. Second Order Analysis

We extend the linear analysis described in the previous section to second order, i.e., quadratic interactions. The interface and field quantities now take the form

$$\begin{aligned} h \cong h^{(0)} + h^{(1)} + h^{(2)} &= h^{(0)}(t) + (H_1 e^{i\mathbf{k}\cdot\mathbf{x}+\lambda t} + c.c.) \\ &\quad + \sum_{m=-2,0,2} H_{2,m}(t) e^{im\mathbf{k}\cdot\mathbf{x}} \\ S \cong S^{(0)} + S^{(1)} + S^{(2)} &= S^{(0)}(z,t) + (\mathcal{S}_1(z) e^{i\mathbf{k}\cdot\mathbf{x}+\lambda t} + c.c.) \\ &\quad + \sum_{m=-2,0,2} \mathcal{S}_{2,m}(z,t) e^{im\mathbf{k}\cdot\mathbf{x}} \\ p \cong p^{(0)} + p^{(1)} + p^{(2)} &= p^{(0)}(z,t) + (P_1(z) e^{i\mathbf{k}\cdot\mathbf{x}+\lambda t} + c.c.) \\ &\quad + \sum_{m=-2,0,2} P_{2,m}(z,t) e^{im\mathbf{k}\cdot\mathbf{x}} \end{aligned}$$

with λ, $\mathbf{k}$, determined by the first order analysis to result in maximum growth rate. The coefficient H_1 can be chosen to be real and if so, as it turns out, the functions $\mathcal{S}_1(z)$, $P_1(z)$, are then also real (see DK02). Quadratic interactions between modes with different wavevectors are excluded because the immediate concern is the mean amplitudes $H_{2,0}$, $\mathcal{S}_{2,0}$, $P_{2,0}$, which depend only on single mode interactions of the form $(Qe^{i\mathbf{k}\cdot\mathbf{x}})(Re^{-i\mathbf{k}\cdot\mathbf{x}})$.

The quantities $p^{(2)}$ and $S^{(2)}$ satisfy

$$\nabla^2 p^{(2)} = -S^{(2)} \qquad z < h^{(0)} \tag{12}$$

$$\nabla^2 S^{(2)} = \begin{cases} 0 & z > h^{(0)} \\ GS^{(2)} & z < h^{(0)} \end{cases} \tag{13}$$

with outer boundary conditions $\partial_z p^{(2)}|_{z=-\infty} = \partial_z S^{(2)}|_{z=-\infty} = 0$ and $S^{(2)}|_{z=h^{(0)}+L} = 0$.

Expand to obtain to second order

$$\mathbf{n} = \frac{1}{\sqrt{1+|\partial_x h|^2+|\partial_y h|^2}} \begin{pmatrix} -\partial_x h \\ -\partial_y h \\ 1 \end{pmatrix}$$
$$\cong \begin{pmatrix} 0 \\ 0 \\ 1 \end{pmatrix} + \begin{pmatrix} -\partial_x h^{(1)} \\ -\partial_y h^{(1)} \\ 0 \end{pmatrix} + \begin{pmatrix} -\partial_x h^{(2)} \\ -\partial_y h^{(2)} \\ -(1/2)(|\partial_x h^{(1)}|^2 + |\partial_y h^{(1)}|^2) \end{pmatrix}.$$

Then $[S] = [\nabla S \cdot \mathbf{n}] = 0$ implies that

$$[S^{(1)}] = 0$$
$$[\partial_z S^{(1)}] = (GS^{(0)}|_{h^{(0)-}})h^{(1)} = \frac{G}{1+F}h^{(1)}$$
$$[S^{(2)}] = -\left(\tfrac{1}{2}GS^{(0)}|_{h^{(0)-}}\right)(h^{(1)})^2 = -\frac{1}{2}\frac{G}{1+F}(h^{(1)})^2 \tag{14}$$
$$[\partial_z S^{(2)}] = (GS^{(0)}|_{h^{(0)-}})h^{(2)} + \left(\tfrac{1}{2}G\partial_z S_0|_{h^{(0)-}}\right)(h^{(1)})^2$$
$$= \frac{G}{1+F}h^{(2)} + \frac{1}{2}\frac{G^{3/2}}{1+F}(h^{(1)})^2. \tag{15}$$

We wish to determine the mean quantities $H_{2,0}$, $\mathcal{S}_{2,0}$, $P_{2,0}$. By averaging (12), (13), and applying the averaged top and bottom boundary conditions we obtain

$$\mathcal{S}_{2,0}(z,t) = \begin{cases} C_{2,0}(t)(1-L^{-1}(z-h^{(0)})) & h^{(0)} < z < h^{(0)}+L \\ \bar{C}_{2,0}(t)\exp[-\sqrt{G}(h^{(0)}-z)] & z < h^{(0)} \end{cases} \tag{16}$$

$$\partial_z P_{2,0}(z,t) = -\int_{-\infty}^{z} \mathcal{S}_{2,0}(s,t)ds$$
$$= -\frac{\bar{C}_{2,0}(t)}{\sqrt{G}}\exp[-\sqrt{G}(h^{(0)}-z)] \qquad z < h^{(0)} \tag{17}$$

for as yet unknown amplitude coefficients $C(t)$, $\bar{C}(t)$. Averaging the interface conditions (14), (15) results in the requirements

$$[\mathcal{S}_{2,0}] = -\frac{G}{1+F}H_1^2 e^{2\lambda t}$$
$$[\partial_z \mathcal{S}_{2,0}] = \frac{G}{1+F}H_{2,0} + \frac{G^{3/2}}{1+F}H_1^2 e^{2\lambda t}.$$

From (16), $[S_{2,0}] = C_{2,0} - \bar{C}_{2,0}$ and $[\partial_z S_{2,0}] = -L^{-1}C_{2,0} - \sqrt{G}\bar{C}_{2,0}$ so that

$$C_{2,0} = -G^{1/2}\frac{F}{(1+F)^2}H_{2,0} - G\frac{2F}{(1+F)^2}H_1^2 e^{2\lambda t} \tag{18}$$

$$\bar{C}_{2,0} = -G^{1/2}\frac{F}{(1+F)^2}H_{2,0} + G\frac{1-F}{(1+F)^2}H_1^2 e^{2\lambda t}. \tag{19}$$

Using $\partial_z^2 p^{(0)} = -S^{(0)}$, $\partial_z^2 p^{(1)} = k^2 p^{(1)} - S^{(1)}$, $p|_h = 0$ at first order, then equation (7) at second order becomes

$$\frac{d}{dt}h^{(2)} = (S^{(0)}|_{h^{(0)-}})h^{(2)} + \left(\tfrac{1}{2}\partial_z S^{(0)}|_{h^{(0)-}}\right)(h^{(1)})^2 + (S^{(1)}|_{h^{(0)-}})h^{(1)} + (k^2\partial_z p^{(0)}|_{h^{(0)}})(h^{(1)})^2 - \partial_z p^{(2)}|_{h^{(0)}}.$$

Averaging and noting (17) results in

$$\begin{aligned}\frac{d}{dt}H_{2,0} &= (S^{(0)}|_{h^{(0)-}})H_{2,0} - \partial_z P_{2,0}|_{h^{(0)}} + ((\partial_z S^{(0)}|_{h^{(0)}}) + (2\mathcal{S}_1|_{h^{(0)-}}) \\ &\quad + (2k^2\partial_z p^{(0)}|_{h^{(0)}}))H_1^2 e^{2\lambda t} \\ &= \frac{1}{(1+F)^2}H_{2,0} + \frac{2\sqrt{G}}{1+F} \\ &\quad \times \left(\frac{1}{1+F} - \frac{\tanh[EF]}{E + (1+E^2)^{1/2}\tanh[EF]} - E^2\right)H_1^2 e^{2\lambda t} \\ &\equiv \delta H_{2,0} + \gamma H_1^2 e^{2\lambda t}\end{aligned}$$

where $E \equiv k/\sqrt{G}$, with solution

$$H_{2,0} = \frac{1 - e^{-(2\lambda-\delta)t}}{2\lambda - \delta}\gamma H_1^2 e^{2\lambda t} \equiv \Gamma_{2,0}H_1^2 e^{2\lambda t} \tag{20}$$

[if $\delta = 2\lambda$ then $H_{2,0}(t) = t\gamma H_1^2 e^{2\lambda t}$]. Thus $H_{2,0}$ grows exponentially with the sign determined by the sign of the coefficient γ. Note that $2\lambda - \delta \cong 0.2944 - (1+F)^{-2}$ which can safely be assumed positive for values of $F = L\sqrt{G}$ relevant here. For large G (thin active layer) and fixed substrate boundary layer thickness L, i.e., the substrate concentration boundary layer is thick compared to the biofilm active region, then $\gamma \cong -2.9712\sqrt{G}(1+F)^{-1} \cong -2.9712L^{-1}$ so that $H_{2,0}$ will be negative thus indicating retardation of mean biofilm growth. As noted, large F is generally the relevant regime for low levels of external shear stress considered in this paper—in the absence of significant bulk fluid flow, substrate advection will generally not be substantial and hence comparatively large diffusive boundary

layers can be expected. The nonlinear analysis presented here predicts, perhaps counterintuitively, that fingering behavior will typically inhibit biofilm growth and substrate uptake. Despite increased biofilm surface area, decreased accessibility of substrate results in reduced growth. Note that in the limit of small F, i.e., a thin substrate boundary layer compared to active region depth, $\gamma > 0$ and hence $H_{2,0} > 0$ so that biofilm growth is enhanced. In this case the increased biofilm surface area is easily visible to the substrate resulting in increased growth. Small F may occur for example in the presence of advective flow in the bulk fluid. However advective flow also results in shear stress so that applicability of the present analysis to the small F regime is unclear. When F is large, however, the substrate source is far from the interface and hence diffusion damps advantageous effects of increased interface area on substrate uptake in the biofilm—this damping goes as $(1 + F)^{-1}$. The dominant effect is an effectively increased barrier to substrate transport through the now nonhomogenous interface region. The effect does not decay with increasing F. Thus fingering would seem to actually reduce overall biofilm growth rate.

4. SUMMARY AND CONCLUSIONS

Considerable speculation has been devoted to the relation between form and function in observed biofilm structure. Why do biofilms sometimes form dense, homogeneous layers and sometimes form complex heterogeneous structures? Such variation is observed not only between different biofilms but also within the same biofilm subject to varying environmental conditions. For example, Stoodley *et al.* (1999a) observed a heterogenous biofilm become thick and homogeneous when exposed to higher glucose concentrations. These structural changes were reversed when glucose concentration was returned to its original level. Similar results were reported in Møller *et al.* (1998). For reasons of practicality, these biofilms are grown under conditions including bulk fluid shear. However structural variations in response to environmental conditions are also observed in biofilms grown in static conditions, e.g., Balaban *et al.* (2003).

Thus a popular suggestion is that biofilm structure varies in response to nutrient availability. For example, Beyenal and Lewandowski (2002) argue that biofilm structure changes to maximize nutrient transport subject to the constraint of resisting exterior bulk flow stress. An obvious possible mechanism for improved intake would be to increase the biofilm–bulk fluid interface area. The basic mechanical model reported here would however seem to indicate that increased interface area can actually inhibit nutrient absorption. While biofilm finger-tops see an improved nutrient environment, a forest of biofilm mushrooms effectively creates a mushy biofilm–bulk fluid layer that slows nutrient transport to the forest floor. This dampening is reversed under sufficiently vigourous bulk flow. Though in that case, mushroom structures become susceptible to shear stress and resulting catastrophic

failure (Stoodley *et al*., 2001). So even in that regime, increased growth may still not provide a true functional advantage.

Nevertheless, exposure of the biofilm undercarriage via heterogeneity may be of benefit even if slowdown of overall growth results. Biofilms attain structural integrity through the EPS matrix (Allison, 2003). Among other properties, the EPS matrix appears to give biofilms viscoelastic constitutive properties that can provide at least some protection from external mechanical stresses (Ohashi and Harada, 1994; Stoodley *et al*., 1999b; Koerstgens *et al*., 2001; Klapper *et al*., 2002; Towler *et al*., in press). Recent work suggests that EPS can degrade under nutrient poor conditions (Stoodley *et al*., 2002; Zhang and Bishop, 2003). Hence, one may speculate that heterogeneous structure (and attendant increased surface area) formed in response to low concentration levels of the limiting nutrient, regardless of effect on overall growth, may serve to improve access of structurally important regions of the EPS matrix to nutrient. Resolution of the connection between biofilm form and function, however, awaits improved understanding of biofilm mechanical properties.

ACKNOWLEDGEMENTS

The author is grateful to Paul Stoodley for helpful discussions. This work was supported by the NIH award 5R01GM067245-02.

REFERENCES

Allison, D. G. (2003). The biofilm matrix. *Biofouling* **19**, 139–150.

Balaban, N., Y. Gov, A. Bitler and J. R. Boelaert (2003). Prevention of *Staphylococcus aureus* biofilm on dialysis catheters and adherence to human cells. *Kidney Int.* **63**, 340–345.

Beyenal, H. and Z. Lewandowski (2002). Internal and external mass transfer in biofilms grown at various flow velocities. *Biotechnol. Prog.* **18**, 55–61.

Breyers, J. D. (Ed.) (2000). *Biofilms II*, New York: Wiley–LISS.

Byrne, H. M. (1999). A weakly nonlinear analysis of a model of avascular tumor growth. *J. Math. Biol.* **39**, 59–89.

Chaplain, M., S. M. Giles and R. J. Jarvis (1995). A mathematical analysis of a model for tumour angiogenesis. *J. Math. Biol.* **33**, 744–770.

Cogan, N. (2003). The role of the biofilm matrix in structural development. *Math. Med. Biol.* (submitted for publication).

Costerton, J. W. (1995). Overview of microbial biofilms. *J. Ind. Microbiol.* **15**, 137–140.

Costerton, J. W., K.-J. Cheng, G. G. Geesey, T. I. Ladd, J. C. Nickel, M. Dasgupta and T. J. Marrie (1987). Bacterial biofilms in nature and disease. *Annu. Rev. Microbiol.* **41**, 435–464.

Costerton, J. W., P. S. Stewart and E. P. Greenberg (1999). Bacterial biofilms: a common cause of persistent infections. *Science* **284**, 1318–1322.

Dockery, J. D. and I. Klapper (2002). Finger formation in biofilms. *SIAM J. Appl. Math* **62**, 853–869.

Eberle, H. J., D. F. Parker and M. C. M. van Loosdrecht (2001). A new deterministic spatiotemporal continuum model for biofilm development. *J. Theor. Med*. **3**, 161–175.

Ermentrout, G. B. (1991). Stripes or spots? Nonlinear effects in bifurcation of reaction-diffusion equations on the square. *Proc. R. Soc. Lond. A* **434**, 413–417.

Greenspan, H. P. (1974). On the self-inhibited growth of cell cultures. *Growth* **38**, 81–95.

Greenspan, H. P. (1975). On the growth and stability of cell cultures and solid tumors. *J. Theor. Biol.* **56**, 229–242.

Heersink, J., W. J. Costerton and P. Stoodley (2003). Influence of the Sonicare toothbrush on the structure and thickness of laboratory grown *Streptococcus mutans* biofilms assessed by digital time-lapse and confocal microscopy. *Am. J. Dentistry* **16**, 79–83.

Heijnen, J. J., C. Picioreanu and M. C. M. van Loosdrecht (1998). Mathematical modeling of biofilm structure with a hybrid differential-discrete cellular automaton approach. *Biotechnol. Bioeng.* **58**, 106–116.

Hermanowicz, S. W. (2001). A simple 2D biofilm model yields a variety of morphological features. *Math. Biosci.* **169**, 1–14.

Klapper, I., C. J. Rupp, R. Cargo, B. Purvedorj and P. Stoodley (2002). A viscoelastic fluid description of bacterial biofilm material properties. *Biotech. Bioeng.* **80**, 289–296.

Koerstgens, V., H.-C. Flemming, J. Wingender and W. Borchard (2001). Influence of calcium ions on the mechanical properties of a model biofilm of mucoid *Pseudomonas aeruginosa*. *Wat. Sci. Technol.* **43**, 49–57.

Kreft, J. U. and J. W. Wimpenny (2001). Effect of EPS on biofilm structure and function as revealed by an individual-based model of biofilm growth. *Wat. Sci. Technol.* **43**, 135–135.

Møller, S., C. Sternberg, J. B. Andresen, B. B. Christensen, J. L. Ramos, M. Givskov and S. Molin (1998). *In situ* gene expression in mixed culture biofilms: evidence of metabolic interactions between community members. *Appl. Env. Microbiol.* **64**, 721–732.

Ohashi, A. and H. Harada (1994). Adhesion strength of biofilm developed in an attached growth reactor. *Wat. Sci. Tech.* **29**, 281–288.

Picioreanu, C. (2000). Multidimensional modeling of biofilm structure. PhD thesis, Delft University of Technology.

Schultz, M. P. and G. W. Swain (1999). The effect of biofilms on turbulent boundary layers. *ASME J. Fluids Eng.* **121**, 44–51.

Stewart, P. S. (2003). Diffusion in biofilms. *J. Bacteriol.* **185**, 1485–1491.

Stoodley, P., I. Dodds, J. D. Boyle and H. Lappin-Scott (1999a). Influence of hydrodyna mics and nutrients on biofilm structure. *J. Appl. Microbiol.* **85**, 19S–28S.

Stoodley, P., Z. Lewandowski, J. D. Boyle and H. Lappin-Scott (1999b). Structural deformation of bacterial biofilms by short term fluctuations in flow velocity: an *in situ* demonstration of biofilm viscoelasticity. *Biotech. Bioeng.* **65**, 83–92.

Stoodley, P., K. Sauer, D. G. Davies and J. W. Costerton (2002). Biofilms as complex differentiated communities. *Annu. Rev. Microbiol.* **56**, 187–209.

Stoodley, P., S. Wilson, L. Hall-Stoodley, J. D. Boyle and H. Lappin-Scott (2001). Growth and detachment of cell clusters from mature mixed species biofilms. *Appl. Environ. Microbiol.* **67**, 5608–6513.

Towler, B. W., C. J. Rupp, A. Cunningham and P. Stoodley (2003). Viscoelastic properties of a mixed culture biofilm from rheometer creep analysis. *Biofouling* (in press).

Wanner, O. and P. Riechert (1996). Mathematical modeling of mixed-culture biofilm. *Biotechnol. Bioeng.* **49**, 172–184.

Wentland, E. J., P. S. Stewart, C.-T. Huang and G. A. McFeters (1996). Spatial variations in growth rate within *Klebsiella pneumoniae* colonies and biofilms. *Biotechnol. Prog.* **12**, 316–321.

Wimpenny, J. W. T. and R. Colasanti (1997). A unifying hypothesis for the structure of microbial biofilms based on cellular automaton models. *FEMS Micro. Ecol.* **22**, 1–16.

Wood, B. D. and S. Whitaker (1999). Cellular growth in biofilms. *Biotech. Bioeng.* **64**, 656–670.

Xu, K. D., P. S. Stewart, F. Xia, C.-T. Huang and G. A. McFeters (1998). Spatial phy siological heterogeneity in *Pseudomonas aeruginosa* biofilm is determined by oxygen availability. *Appl. Environ. Microbiol.* **64**, 4035–4039.

Zhang, X. and P. L. Bishop (2003). Biodegradability of biofilm extracellular polymeric substances. *Chemosphere* **50**, 63–89.

Received 27 May 2003 and accepted 6 November 2003